EFFECTS OF MUSSEL SHELL AGGREGATES ON HYGRIC BEHAVIOUR OF AIR LIME MORTAR AT DIFFERENT AGES

Martínez-García, Carolina[1]; González-Fonteboa, Belén[2]; Carro-López, Diego[3]; Martínez-Abella, Fernando[4]

[1]**PhD Student at the School of Civil Engineering**. Department of Construction Technology, University of A Coruña. **Postal Address**: E.T.S.I. Caminos, Canales, Puertos. Campus Elviña s/n, 15071 La Coruña, Spain. **E-mail**: carolina.martinezg@udc.es. **Telephone number**: (+34) 881015463. **Fax**: (+34) 981167170

[2]**Associate Professor at the School of Civil Engineering**. Department of Construction Technology, University of A Coruña. **Postal Address**: E.T.S.I. Caminos, Canales, Puertos. Campus Elviña s/n, 15071 La Coruña, Spain. **E-mail**: bfonteboa@udc.es. **Telephone number**: (+34) 881011442. **Fax**: (+34) 981167170

[3]**Associate Professor at the School of Civil Engineering**. Department of Construction Technology, University of A Coruña. **Postal Address**: E.T.S.I. Caminos, Canales, Puertos. Campus Elviña s/n, 15071 La Coruña, Spain. **E-mail**: diego.carro@udc.es. **Telephone number**: (+34) 881015433. **Fax**: (+34) 981167170

[4]**Professor at the School of Civil Engineering**. Department of Construction Technology, University of A Coruña. **Postal Address**: E.T.S.I. Caminos, Canales, Puertos. Campus Elviña s/n, 15071 La Coruña, Spain. **E-mail**: fmartinez@udc.es. **Telephone number**: (+34) 881011443. **Fax**: (+34) 981167170

Abstract

Mussel shells, composed of calcium carbonate (> 95%) and organic matter, are suitable alternatives to conventional sand in mortar. In addition, the use of lime instead of cement as a binder has also been considered for sustainable construction materials as well as in restorative applications.

This study aims to contribute to the knowledge of air lime mortar through the analysis of the water transport properties of air lime mortar produced with mussel shell aggregates at different ages. Four mortar groups were obtained from the reference mortar by replacing limestone sand with mussel shell sand at substitution rates of 25%, 50%, and 75%. Water absorption, capillary uptake, weight variation, and drying from the fresh state up till one and two years were determined. The organic matter content and flaky seashell shape are responsible for the main differences observed between the mussel mortars

and reference mortar. These two characteristics promote transport tortuosity paths and hydrophobic behaviour leading to reduced capillary uptake and increased drying resistance index. Furthermore, they enhance water retention, which increases the carbonation rate.

Keywords:

Coating mortars; water absorption; capillarity uptake; drying index; tortuosity

Highlights:

- Mussel shell content changes capillary absorption rate with ageing.
- Tortuosity path in capillary absorption are analysed.
- Carbonation is analysed with weight variation.
- Different velocities in weight variation respect to control mortar are shown.
- Mussel shell particles affects drying behaviour in air lime mortars.

1 INTRODUCTION

The feasibility of using various types of seashell aggregates in concrete [1–5] and cement mortar [6–10] has been studied in recent years. Seashells such as mussel, periwinkle, oyster, and scallop can be suitable alternatives to conventional sand in the development of new sustainable building materials.

The microstructure of seashells, including mussel shells, is mainly formed by calcium carbonate (> 95%) with traces of organic matter. This organic matrix composite of polysaccharides (chitin), proteins, and glycoproteins are presented mainly at the outer and inner layers of the mussel shells (periostracum and nacre, respectively). The small organic matter content and flaky shape of seashells are responsible for most of the changes observed in the behaviour of lime and cement matrix [11–14].

Various studies have analysed the use of additives that contain proteins, polysaccharides, and fatty acids in lime mortar. A recently published study [15] demonstrated that natural polymers, such as milk products, casein, organic fat, rice, plant saps, and various herbs, increased the durability of plasters of different heritage building in several countries.

Traces of sticky rice, Tung oil, and animal blood were detected in ancient lime mortar [16–20]. Replications of these ancient mortar confirm that sticky rice accelerates the setting and hardening times and increases the compressive strength and bonding capacity of lime mortars [16,20]. Mortars prepared with Tung oil possesses improved mechanical properties, water resistivity (reduction of water sorption), and weather resistance than reference mortar [16,17]. Lime mortar containing animal blood possesses enhanced hardening, binding strength, waterproof property, weather resistance, and curing speed than conventional lime mortar [16,19]. Oxblood proteins have an inhibiting effect on calcite formation, which could induce a slower initial carbonation rate [18].

In the study by Ventolá et al. [21], nopal, animal glue, casein, and olive oil were used as additives in restoration lime mortar. The results pointed out that mortars containing organic additives exhibited enhanced mechanical properties and water resistance and change carbonation speed. Sugarcane bagasse ash [22] mixed with lime was used as a replacement of cement for stabilisation of compressed soil blocks and presented an excellent binder alternative with low energy consumption.

Nunes et al. [23–25] investigated the effect of linseed oil in lime mortar, which exhibited a water-repellent behaviour and air bubbles related to entrained air during mixing. The findings reveal that mortars produced with organic additives displayed reduced capillarity and high resistance to freeze-thaw cycles. Lime mortar made with linseed oil, containing other organic additives, such as brown sugar and cow milk, was studied by Centauro et al. [26]. They observed transformations induced by the additives: hydrophobic effect, different distributions and shapes of macropores, and different levels of carbonation.

Various materials, such as an extract of natural polymer (areca nut) or spent cooking oil and albumen, have been added in restorative lime mortars [27,28]. The results demonstrate that mortar containing

the organic extract showed delayed drying and setting processes, decreased water absorption and capillarity, increased carbonation rate, and improved mechanical and durability properties. Spent cooking oil addition induced hydrophobic characteristics, and albumen addition increased the setting kinetics of mortar.

In a previous study [14], different properties of air lime coating mortar with mussel shell replacing limestone sand were investigated. These properties were evaluated at only a single age, i.e. one year, using two binders: lime putty and hydrated lime. Mussel shell flaky particles and the presence of organic matter introduced a high volume of large pores in the air lime mortar and changed the pore size distributions. The carbonation degree of lime putty mortar significantly increased with the mussel shell content. This increase was also observed in hydrated lime mortars but to a lower extent. Finally, the mechanical strength decreased in mussel shell mortar due to the higher porosity and weaker bond between mussel shell particles and air lime paste.

An important advantage of applying coatings in buildings is moisture reduction inside the structure [29]. Usually, mortars deteriorate due to moisture and water movement inside of the pore structure. The penetration of water can favour the entry of salts, which can damage mortars and cause severe durability risks [30]. Generally, coating mortars lead to easy and accelerated evaporation of water entering the mortar, high flexibility, excellent adhesion, and compatibility with the support [31]. Adequate knowledge of different mortar-coating characteristics (pore system, hygric, and physicomechanical properties) are required to predict mortar durability.

This study aims to contribute to knowledge of the behaviour of air lime mortar through the analysis of water transport properties of lime mortar produced with mussel shell aggregate. Therefore, water transport properties were analysed in this study by determining the water absorption, capillary uptake, weight variation, and fresh-state drying of air lime mortar from one to two years.

2 MATERIALS AND MIXES

Four groups of mortar were prepared with slaked lime putty (PL), having a water content of 64% by weight (EN 459-1 CL90-PL). The composition from X-ray fluorescence (XRF) analysis showed a 70.5% CaO content, and the loss on ignition at 975 °C was 22.6%. In addition, the calcium carbonate ($CaCO_3$) and calcium hydroxide ($Ca(OH)_2$) contents were calculated from the TGA results, which were 7.41% and 88%, respectively.

Two types of aggregates were used: limestone sand (LS) and mussel shell sand (MS). MS was obtained from mussel shells after heat-treating in a trommel rotary screen at 135 °C for 32 min. MS was supplied, after a crushing and sieving process, in two different size fractions: coarse sand (CMS, 0-4 mm) and fine sand (FMS, 0-1 mm). These two fractions were combined (88.5% of FMS with 11.5% of CMS) to obtain MS with a maximum size of 2 mm and a fineness modulus of 2.21 (appropriate for producing coating mortar). Particle density of CMS and FMS was 2.65 and 2.73 kg/dm^3 respectively. LS was sieved to four different size fractions: 0-63µm, 63µm-0.25mm, 0.25-1mm, 1-4mm. Afterwards, these fractions were combined to obtained a LS with a particle size distribution similar to that of MS. The LS obtained presented maximum size of 2 mm, fineness modulus of 2.23 and a particle density of 2.67 kg/dm^3.

XRF results indicate that mussel shells are composed of mainly calcium carbonate (95%), silicon oxide (2%), and sodium oxide (0.4%), which can be related to the presence of sodium chloride in the samples. Shells are formed by the bio-mineralisation of $CaCO_3$ with a small amount of organic matrix holding the structure together. Mussel shells are divided into three parts: the outer layer (periostracum), the middle layer (prismatic layer), and the inner layer (nacre). The central and thickest layer has a prismatic structure with an array of parallel calcite prisms. Both the external and internal layers mainly consist of protein. The organic matter content present in the CMS and FMS were 1.49% and 2.15%, respectively. A more detailed characterisation of the binder and aggregates has been already published [12–14].

In this experimental setup, four mortar groups were obtained from a reference mortar PL0 by replacing LS with MS for substitution rates of 25%, 50%, and 75% (PL25, PL50, and PL75). After several trials, a

binder-to-aggregate ratio of 1:2.5 (by volume) was selected. Table 1 shows the mix proportions (by weight) of both the reference and mussel shell mortars.

Table 1. Lime-putty mortar dosages by weight (g/l).

Substitution rate (%)	PL0	PL25	PL50	PL75
Lime putty (with 64% water content)	629.1	629.1	629.1	629.1
Limestone sand (LS)	1270.3	952.7	635.1	317.6
Mussel shell sand (MS)	0	323.52	647.03	970.55

The mortars were mixed based on UNE-EN 196-1 specifications and cast in prismatic moulds (40 mm × 40 mm × 160 mm) and cylindrical PVC tubes of 150 mm diameter and 20 mm thickness following UNE-EN 1015-11 guidelines. The mixes were manually compacted with a 50 g rammer. The samples were cured inside a climatic chamber (20 ± 2 °C and 60±5%) for 5 days before demoulding, with a standard CO_2 concentration. All the tests were carried out at different ages.

3 TEST METHODS

3.1 Water absorption after immersion and boiling

Water absorption was carried out according to UNE 83980 recommendations. At least three specimens were taken from each cylindrical sample of hardened lime mortar at 28 days, 120 days, and 1 year. Water absorption after immersion and after immersion and boiling were obtained.

3.2 Capillary water absorption

Water absorption by capillarity test was determined following UNE-EN 15801 specifications. This test was conducted at 40 days, 200 days, and 2 years.

Three 40x40x160 mm samples of each mortar were used for this test. Dried samples were broken (from a flexural test) into two halves, and the tested surface (the smooth face of 40x40 mm) was polished and dry-cleaned. Then, their dry weights were measured (m_0). Therefore, six pieces of each mortar were tested. The pieces were placed such that the tested face turned down on a tray with a wet layer of 5

mm width filter paper. The specimens were taken from the tray after 10 min, and the surface water was quickly removed with a damp cloth, weighed (m_i), and immediately introduced again into the tray. This procedure was repeated several times for 72 h.

The capillary absorption at each period was calculated as the absorbed water divided by the surface area (kg/m^2):

$$Q = \frac{m_i - m_0}{A} \quad (1)$$

A: surface area, (m^2)
m_i: weight at time t_i, (kg)
m_0: dry weight, (kg)
Q_i = capillary absorption at time t_i, (kg/m^2)

These values were represented as a function of the square root of time (in min). The capillary water coefficient (C in kg/(m^{2}min$^{0.5}$)) was calculated as the slope of the initial linear section of the curve (from the origin until 2 h). It expresses the initial speed of capillary absorption. The asymptotic values at 72 h were also measured.

Considering that a theoretical preferential orientation of mussel shell particles can occur in mussel mortar, besides the standard procedure, capillary tests were performed in two additional directions. One more batch with three sample of each mortar was prepared for this purpose. Samples were placed with the long side of the prisms (80 mm × 40 mm) in contact with water: first, positioned parallel to the cast direction, and second, perpendicular to the cast direction. The tested faces were polished and dry-cleaned before placing over the wet filter paper, and the procedure was the same as that described previously. This test was carried out after 90 days and after 2 years.

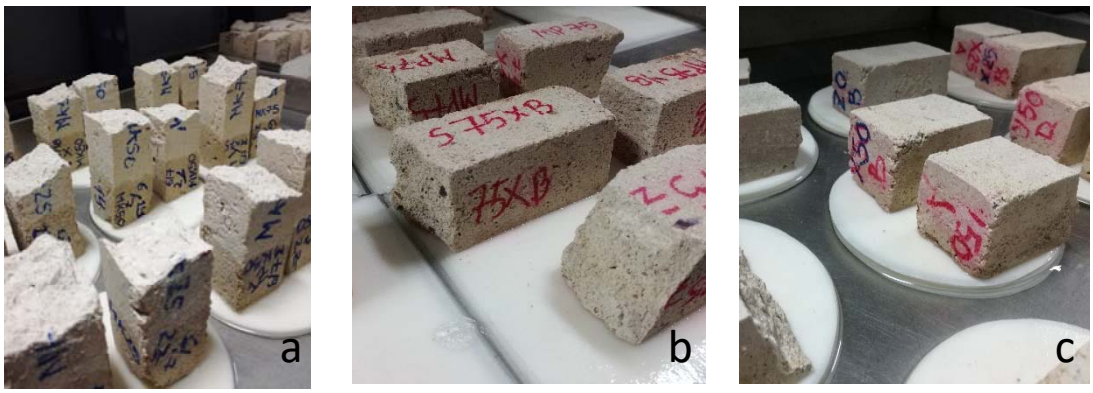

Figure 1. Capillary test: a) standard test, b) specially designed test – parallel to cast direction, c) specially designed test – perpendicular to cast direction.

3.3 Drying test

Drying test was determined according to UNE-EN 16322 recommendations. The test was performed in both fresh and hardened states. Fresh mortar mixes were introduced into a PVC tube of 150 mm diameter and 20 mm thickness that laid on a plastic mesh. Mortar was cast up to the top of the tube, and the tube was removed. The mortar samples were left to dry throughout the whole surface area on the mesh. The weights were measured from demoulding until one year when the carbonation process was already in progress. The samples were weighed several times per day in the first week. Subsequently, they were weighed once a day, once a week, and once a month up to nine months.

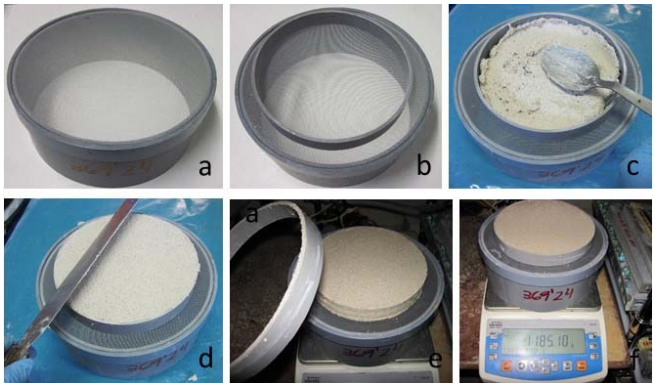

Figure 2. Drying test in fresh state: a) plastic mesh, b) PVC tube, c) casting, d) levelling, e) demoulding, f) weighing.

Hardened-state drying test was performed at 50 and 200 days after the capillary test was conducted, using the same samples used in capillary tests (40x40x160 mm). The samples were placed in a mesh tray and kept in a climatic chamber (20 ± 2 °C and 60±5%) until a constant mass was obtained. The samples were weighed several times each day during the first 48 h and daily (once a day) after that, up to 8 days, when all the samples achieved equilibrium with the environmental conditions.

In the fresh state, results relating the variation of mass with time (square root in h) were obtained. Mass variation was calculated from the mass difference at every instant during the test concerning the initial mass. In this state, two stages were considered: the first stage where water evaporation was predominant and weight loss was recorded, and the second stage where carbonation was prevalent and weight increase was measured.

In hardened state, the drying curve was plotted, relating the square root of time (in hours) in the abscissae and the water content per mass concerning the sample mass in dry state (%) in the ordinate. The water contents (M_i) of the samples were determined using the following equation:

$$M_i = \frac{m_i - m_d}{m_d} \times 100 \quad (2)$$

M_i (%): water content at time t_i
m_i (kg): the sample mass during the drying process at time t_i
m_d (kg): the sample mass in dry state conditions
The drying index (DI) was calculated, as follows:

$$DI = \int_0^{\mathrm{f}} \frac{M_i . \mathrm{dt}}{M_{max}.t_f} \quad (3)$$

M_i (%): water content at time t_i
M_{max} (%): maximum water content
t_f (h): lasting time of the test. The final testing time considered was 145 h.

4 RESULTS AND DISCUSSION

4.1 Water absorption

The results of the water absorption after immersion (AI) and after immersion and boiling (AIB) of all the mortars are presented in Figure 3.

PL0 and PL25 have the same water absorption values at all ages after immersion, and the differences are low after immersion and boiling. Generally, water absorption is higher in mussel shell (MS) mortar than in reference mortar at all ages owing to the high volume of air voids introduced by the MS particles, as stated in a previous study [14]. The values obtained for PL75 at 28 days are not presented in Figure 3 because the results are considered invalid due to material loss at this age. This material loss is produced because portlandite can be dissolved in water at early ages due to low carbonation. This effect is comparatively noticeable in mortar with high MS aggregate content because of its higher porosity and weaker bonding with air lime matrix.

Overall, all mortars show a decrease in water absorption as carbonation progresses, due to porosity reduction.

AIB is higher than AI in all MS mortars. Boiling allows the water that could not initially penetrate through immersion because of the barrier effect of the MS particles to fully penetrate the pores.

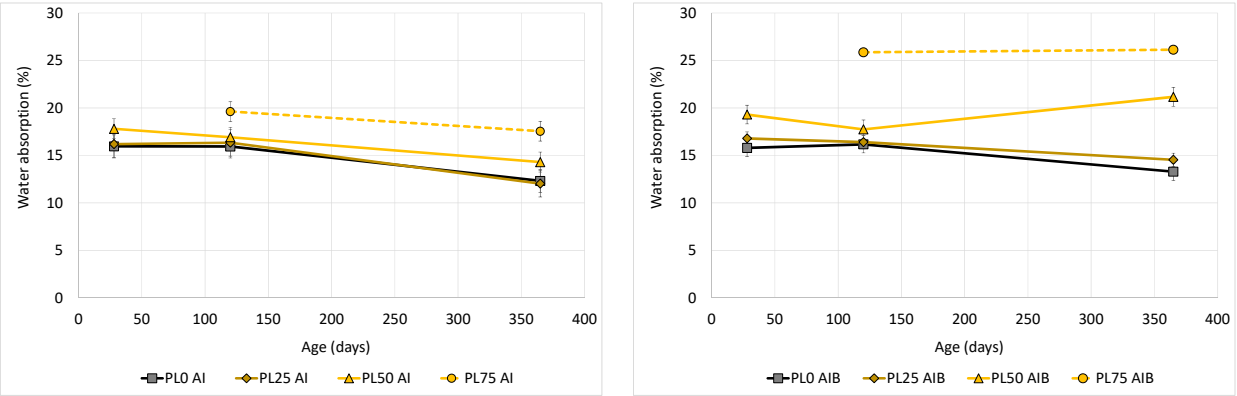

Figure 3. Water absorption at 28 days, 120 days and 1 year.

4.2 Capillary uptake

Sorptivity is a critical factor that indicates the mortar service life in binding materials, as it controls the ingress of moisture and soluble salts. Therefore, the capillary uptake of lime mortar was measured at 40 days, 200 days, and 2 years, as shown in Figure 4. Capillary uptake sets the water absorption kinetics of lime mortars. Capillary coefficient and asymptotic values (at 72 h) are calculated from the curves and are shown in Figure 5 and Figure 6, respectively.

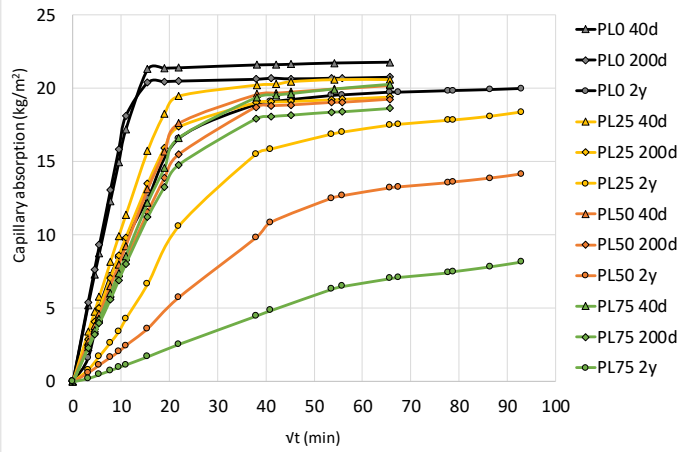

Figure 4. Capillary uptake at 40 days, 200 days, and 2 years.

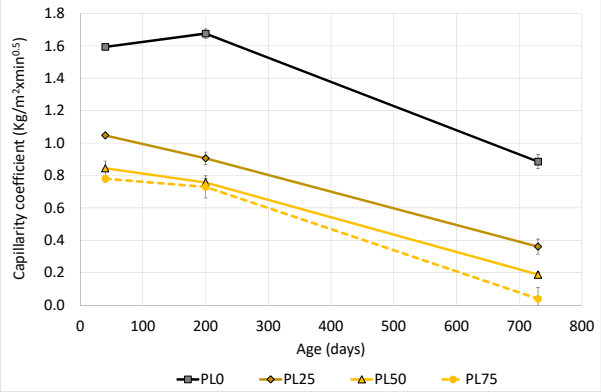

Figure 5. Capillary coefficient at 40 days, 200 days, and 2 years.

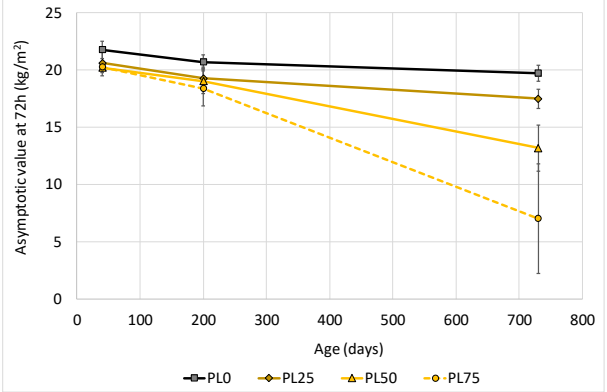

Figure 6. Asymptotic value at 40 days, 200 days, and 2 years.

The water absorption rate (represented by the capillary coefficient, that is, the slope of the capillary uptake curve) and total water absorbed by capillarity (characterised by the asymptotic value obtained

at 72 h) are lower in MS mortar than in reference mortar. Additionally, the values of both capillary coefficient and total water absorbed by capillarity decrease with aging, with the lowest values obtained for MS mortar having 75% mussel aggregate content.

Therefore, an increase in MS content leads to a lower capillary absorption rate at all ages. The decrease observed at two years was the highest, because the carbonation was almost completed, and the samples had a significant porosity reduction. In this case, not only was the water absorption rate lower but also, the total water absorbed was considerably lower than at 40 days. Similarly, the reduction is more noticeable in PL75.

These results are due to different reasons. MS incorporates organic matter (polysaccharides) into its structure, and these polysaccharides reform the hydrophilic capillary surfaces into hydrophobic surfaces owing to their hydrocarbon structure [32]. Other authors [17,19–21,23,26,27] report that different polysaccharides restrict the pores responsible for capillary rise. Hence, organic matter can enhance mortar durability when it acts as a water repellent.

Mortar pore structure is also a significant factor that influences hygric properties. Capillary sorptivity force increases when the pore diameter decreases. Therefore, pores ranging between 10 and 100 μm (present in MS mortars [14]) may influence the amount of water absorbed during the free water absorption test (Figure 3). However, these large pores have less effect on the total water uptake by capillarity, as PL75 yields the lowest water absorbed by capillarity. Upon aging, the reduction in the total water uptake is noticeable, particularly in PL75, due to the high rate of carbonation development exhibited by this mortar at 365 days [14].

In addition, the higher water absorption rate observed in the reference mortar suggests that pores with diameters between 0.1 and 1 μm have a significant effect on capillary uptake, as this mortar has a larger pore volume. The differences in the volume of these pores (i.e. between reference mortar and MS mortars) do not change with aging; therefore, the differences in the water absorption rate are also the same at 40 and 365 days.

Furthermore, the water absorption kinetics of lime-mussel mortars is probably influenced by the flaky shape of MS particles. This property may allow mussel particles to act as barriers to water uptake by capillarity as they create transport tortuosity paths. The tortuosity of the water flow path in mortar depends on different parameters, such as binder type, water-to-binder ratio, and aggregate volume fraction [33]. However, aggregate volume fraction has the most significant effect on water transport tortuosity. Tortuosity has been studied using numerical approaches [34–36], but there is no direct experimental method to measure it [37]. In granular media, the main parameters that affect tortuosity are particle shape, packing method, and angularity [38]. Flaky angular mussel particles provide high aggregate volume fraction and thus increase tortuosity.

To confirm tortuosity paths in mussel mortar, as aforementioned (3.2) a capillary test was performed by placing mortar samples in two different positions. First, the samples were positioned parallel to the cast direction, and second, perpendicular to the cast direction.

It is supposed that the mussel particles would develop a preferential orientation perpendicular to the cast direction. If this assumption is correct, then the capillarity curves will be different in both tests. When the samples are positioned perpendicular to the cast direction, the particle orientation will restrict water uptake as it will promote the tortuosity of the water paths. On the contrary, when samples are placed parallel to the cast direction, the particles will be oriented parallel to water flow, promoting capillary water rise (Figure 7).

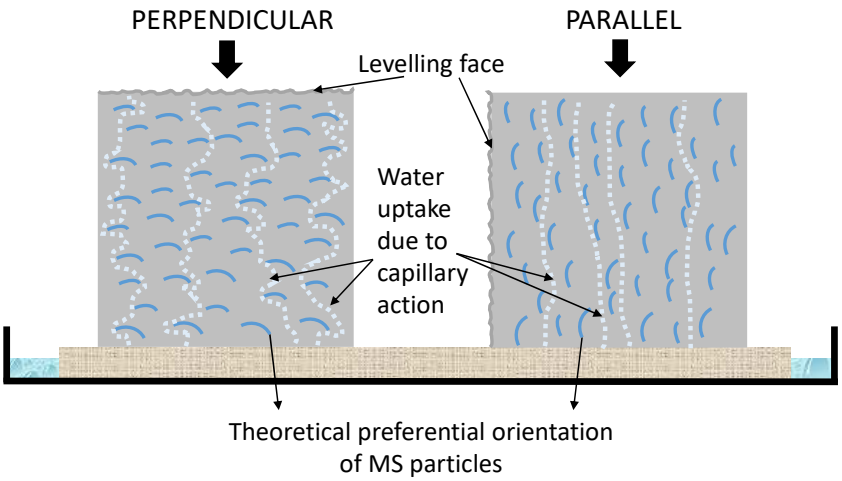

Figure 7. Water uptake test. Perpendicular to cast direction (left) and parallel to cast direction (right).

The results displayed in Figure 8 confirm that reference mortar hardly presents differences in both curves; if placed parallel or perpendicular to the cast direction, the obtained curves are similar at any age. Conversely, at both 90 days and 2 years, MS samples positioned parallel to the cast direction show capillary curves with higher slope and asymptotic value than samples placed perpendicular to the cast direction. The differences are more pronounced in mussel mortars with high replacement percentages and at 2 years. Tortuosity water paths become more significant as the mussel aggregate content increases. In addition, the differences are higher at older ages, when carbonation is almost completely developed, porosity is low, and water transfer is only controlled by interconnected capillary pores. In this case, the effect of tortuosity paths on the pore network is highly significant.

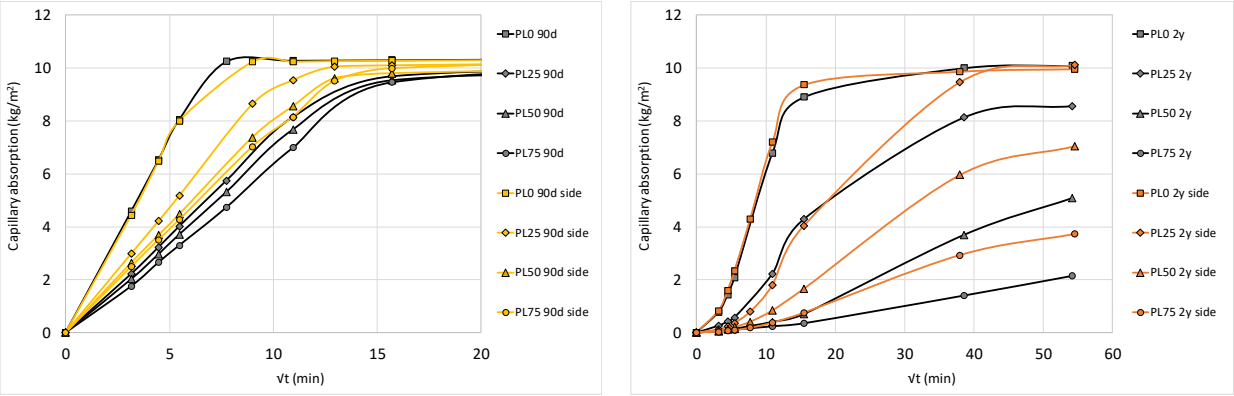

Figure 8. Capillary curves in samples placed parallel and perpendicular to cast direction, at 90 days age (left), 2 years (right).

4.3 Weight variation from fresh state

The weight variation from the fresh state was analysed based on a standard drying test (see section 3.3), and the results are presented in Figure 9 and Figure 10. As all the mortars were prepared with the same amount of kneading water, and drying was ensured under the same external conditions, the observed differences were owing to MS content.

Two predominant stages occur in the fresh state. The first stage takes place just after mixes are produced, and a certain amount of kneading water evaporates, decreasing the mortar weight. Once this kneading water is about to evaporate completely [39], the second stage (carbonation) starts to predominate. This carbonation process is detected by an increase in the weight of samples caused by the transformation of portlandite into calcite, which also involves an increase in the solid volume [40]. The optimum water content for carbonation is achieved when it corresponds to the maximum adsorption on the pore surface before extensive capillary condensation occurs [21].

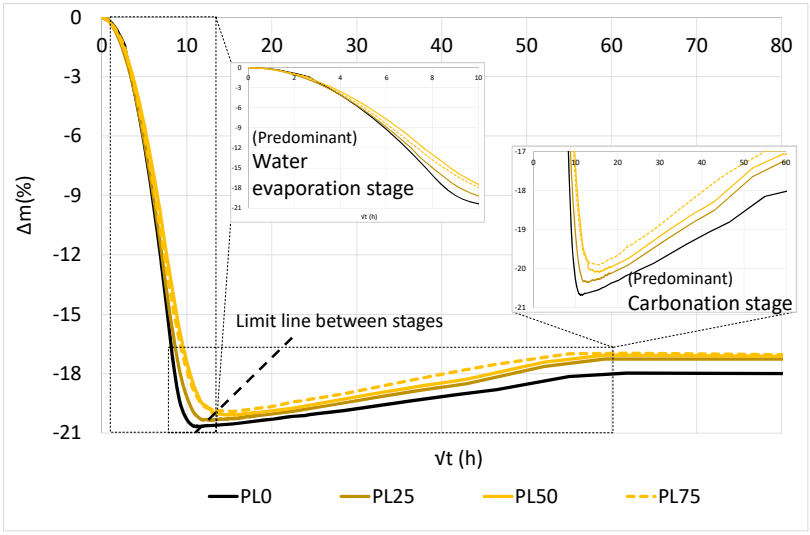

Figure 9. Weight variation from fresh state until 9 months.

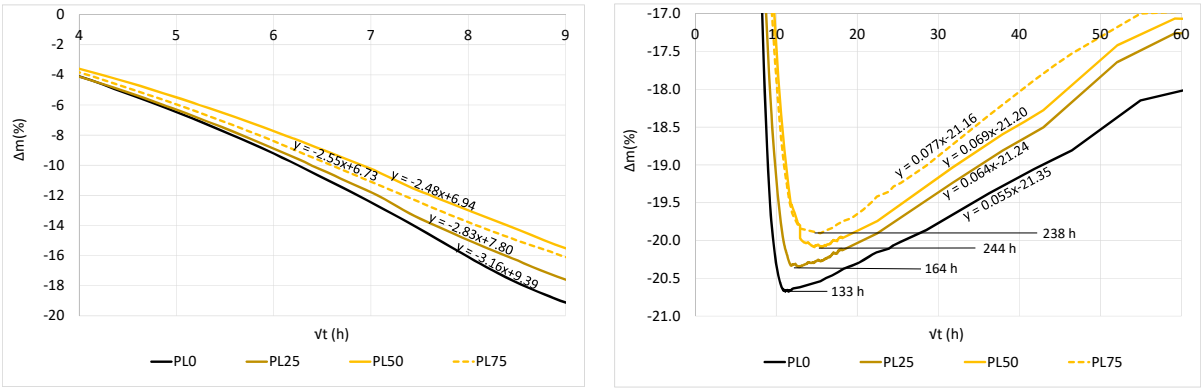

Figure 10. Details of the two predominant stages in weight variation from fresh state: water evaporation stage (left) and carbonation stage (right).

Table 2. Data of weight variation curves for fresh state.

	Maximum time Δm (h)	Slope of the curve at water evaporation stage	Slope of the curve at carbonation stage
PL0	133	-3.16	0.055
PL25	164	-2.83	0.064
PL50	244	-2.48	0.069
PL75	238	-2.55	0.077

Reference mortar gave the highest value of total weight variation; thus, the higher the MS content in mortar, the lower the weight variations. However, these maximum values are reached at different periods for each mortar. The reference mortar first reaches the maximum value at 5.5 days, while PL50 and PL75 take nearly twice the time to reach their respective maximum values (10 days).

During the first stage, when water evaporation predominated, the slope of the curves (Table 2) indicates that the drying rate is lower for higher MS aggregate content. Nevertheless, during the second stage where carbonation is prevalent, the slope (Table 2) increases with MS content. Hence, a higher MS aggregate content results in a more rapid carbonation rate.

These two findings demonstrate that MS promotes moisture retention in lime mortar due to the water blockage effect of the particles and/or the hydrophobicity of organic matter content [27,41]. This water retention decreases water evaporation, delaying the initiation of the carbonation process. However, once carbonation begins, water retention increases the moisture content in the pore structure, and together with the high volume of large pores (> 10 μm) that allows for greater access to CO_2 diffusion [42], increases the carbonation rate. This effect of organic matter on carbonation development has also been observed in other studies [16,18,21,27].

4.4 Drying in hardened state

As was stated in the literature [25,42–44], drying occurs in different stages. The first drying stage (stage I) comprises transport of liquid water to the surface, followed by evaporation. At this stage, the moisture content approximately decreases linearly with time; this is why this stage is also called ‘constant drying rate period. During this period (or a film of water exists on the surface, or surface pores are saturated enough to produce a similar effect), the drying rate is mostly controlled by the surrounding environmental conditions rather than solid moisture profile [42].

The second drying stage (stage II), named as ‘falling drying rate period’, is characterised by a decrease in the liquid water transport and an increase in the water vapour diffusion limited by intrinsic characteristics of the material. At this stage, the drying rate falls, which is expressed in the concave form

of the drying curve (the evaporation front recedes into the material) [25]. Azenha et al. [42] state that at this stage, the rate at which water is supplied to the body surface due to capillarity becomes less than the rate at which liquid evaporates. Consequently, the global drying rate decreases during this stage.

The drying test was performed at 50 and 200 days. The drying curves are shown in Figure 11, and the drying resistance indexes (Di) obtained from the curves are presented in Figure 12. The drying index was calculated considering 145 h as the final testing time and reflects the global drying evaluation, considering both drying stages, liquid water transport, and water vapour diffusion. The higher the drying resistance index, the more difficult it becomes for the material to lose water [44,45].

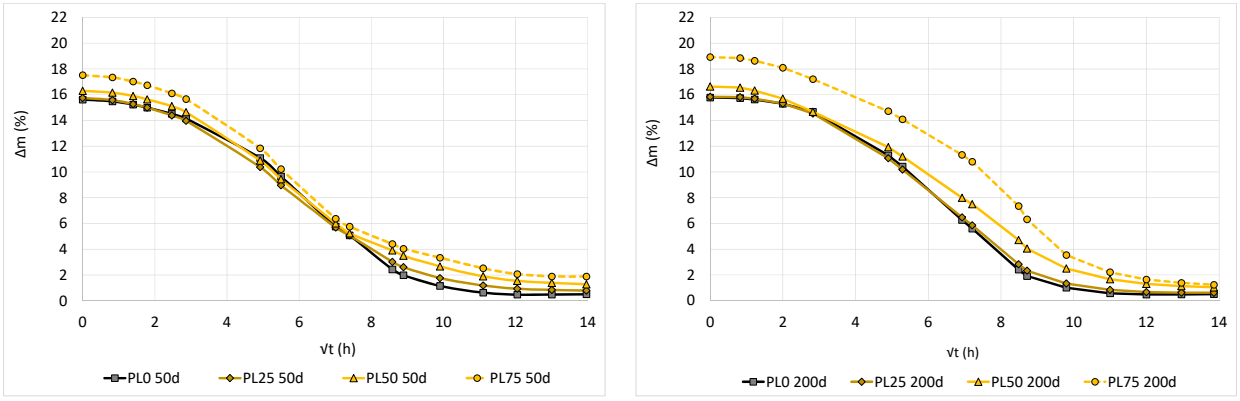

Figure 11. Drying curves at 50 (left) and 200 days (right).

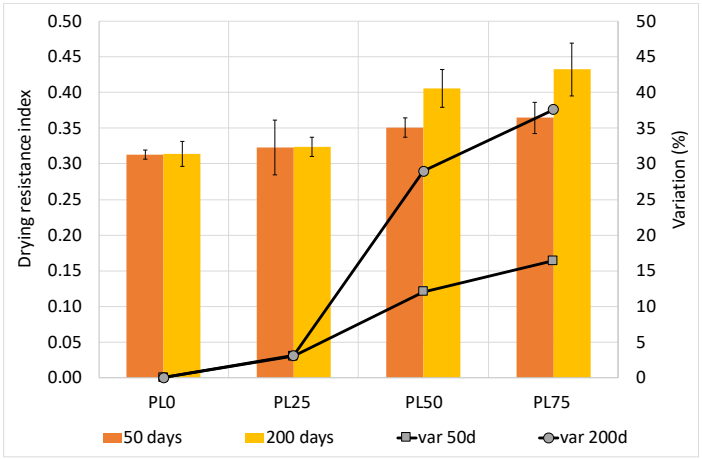

Figure 12. Drying resistance index of lime mortars at 50 and 200 days.

In hardened state, MS mortars exhibit a different drying behaviour compared to the reference mortar at both ages. MS mortars show inferior drying behaviour than the reference mortar; all the curves over the reference mortar curve at all ages. Therefore, the drying resistance index is higher for MS mortars than the reference mortar at all ages.

Differences in the drying index of MS and reference mortars are lower than those detected in capillary uptake at both ages. The major factor that affects drying is the blockage effect of flaky mussel particles, as the high volume of large pores (which hinders capillary uptake in mussel mortars) promotes drying. Additionally, the presence of polysaccharides and proteins (chitin) helps in the retention of water in mussel lime mortar [19,27,41].

Ageing hardly affects the drying of the reference and PL25 mortars, but mortars with high replacement percentages exhibit higher drying resistance with age. The carbonation rate between 50 and 200 days is expected to be higher in MS mortars with high replacement percentages, as observed from the results of weight variation from the fresh state. This suggests that volume reduction of large pores owing to carbonation between 50 and 200 days may be more noticeable in MS mortars than the reference mortar. This reduction worsens the drying capacity, leading to the increase in drying resistance index, especially in mortars with high MS content.

At both ages, MS mortar curves do not reach the zero value along the *x*-axis, which means that these mortars still exhibit moisture retention at the final testing period. Moreover, a higher mussel shell content results in increased water retention at the end of the test. This result again confirms the weight variation measurements, which are due to flaky particles and the chitin effect [27].

Furthermore, in lime mortars, there is a clear relationship between capillary coefficient and drying index [45]; that is, the faster the capillary absorption, the easier the global drying and vice versa. This statement is in agreement with the obtained results (Figure 13). A higher MS content leads to a lower

capillary coefficient and higher drying resistance index. As mentioned earlier, this relationship is nonlinear because MS content influences capillary absorption to a greater extent than drying behaviour.

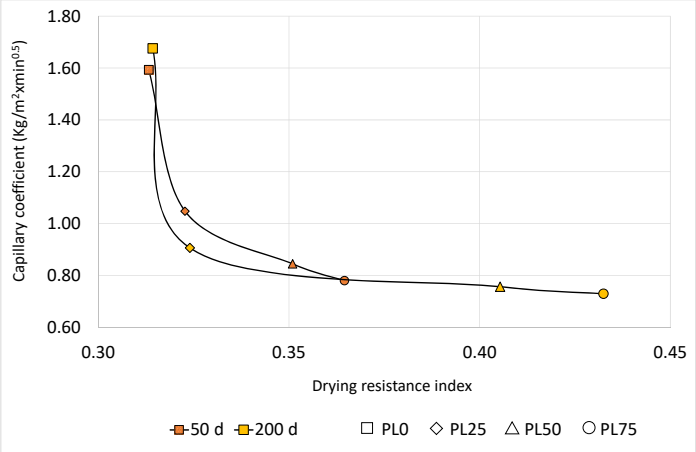

Figure 13. Capillary coefficient vs. drying index.

5 CONCLUSIONS

In this study, the effect of replacement of conventional sand with mussel shell sand in coating mortars that incorporate lime putty (PL) as binder material is analysed. Sand was replaced with mussel shell aggregate at different substitution rates (25%, 50%, and 75%). Water transport properties were analysed upon ageing, and the most significant conclusions are summarised as follows:

- Mussel mortar exhibits higher water absorption at all ages due to increased porosity caused by the introduction of air voids by organic matter content and flaky particle shape. Water absorption after immersion decreases with ageing, owing to porosity reduction that involves carbonation showing all mortars similar evolution.
- An increase in mussel shell content leads to lower capillary absorption rates at all ages. The water absorption rate is not only lower but also, the total water absorbed by capillarity is considerably lower. This lower capillarity absorption is caused by different factors: the hydrocarbon structure of polysaccharides present in mussel particles may change the

hydrophilic surfaces of the capillaries into hydrophobic surfaces acting as a water-repelling agent; large pores ranging between 10 and 100 µm sizes introduced by mussel particles reduce the amount of water absorbed by capillarity; the flaky shape of mussel particles acts as a barrier to water uptake by capillarity, as it creates transport tortuosity paths. Upon aging, the reduction of the total water uptake is more noticeable in mussel mortars because of the high carbonation developed by these mortars at 365 days.

- The addition of mussel aggregate influences the weight variation of mortar. The findings demonstrate that mussel shell promotes water retention. Therefore, in mussel mortars, the weight loss due to evaporation is delayed, and the total water loss is lower than in the reference mortar. On the contrary, the rate of weight gain during the carbonation stage is higher. The carbonation process will be significantly affected by the presence of mussel shell particles.
- Mussel mortars show higher drying resistance index than the reference mortar at all studied ages due to the blockage effect of flaky mussel particles and the presence of organic compounds that enhance water retention. The higher reduction of large pores owing to carbonation in mussel mortars with high replacement rates worsens the drying capacity, leading to a noticeable increase in these mortars, and the drying resistance index at 200 days.

6 ACKNOWLEDGEMENT

This work has been carried out within the framework of the following projects: “Assessment of Galician bivalve shell in the construction sector”; Code 00064742 / ITC-20133094, funded by CDTI under the FEDER-Innterconecta Program, and co-financed with European Union ERDF funds and “Sustainable High Performance Self Compacting Concrete using low clinker cement and internal curing and self healing agents”; Code BIA2017-85657-R funded by MINECO.

7 REFERENCES

[1] M. Olivia, A.A. Mifshella, L. Darmayanti, Mechanical properties of seashell concrete, in: Procedia Eng., 2015. doi:10.1016/j.proeng.2015.11.127.

[2] Monita Olivia; Revina Oktaviani; Ismeddiyanto, Properties of concrete containing ground waste cockle and clam seashells, Procedia Eng. 171 (2017) 658–663.

[3] D.H. Nguyen, M. Boutouil, N. Sebaibi, F. Baraud, L. Leleyter, Durability of pervious concrete using crushed seashells, Constr. Build. Mater. 135 (2017) 137–150. doi:10.1016/j.conbuildmat.2016.12.219.

[4] C. Varhen, S. Carrillo, G. Ruiz, Experimental investigation of Peruvian scallop used as fine aggregate in concrete, Constr. Build. Mater. 136 (2017) 533–540. doi:10.1016/J.CONBUILDMAT.2017.01.067.

[5] J. Wang, E. Liu, L. Li, Characterization on the recycling of waste seashells with Portland cement towards sustainable cementitious materials, J. Clean. Prod. 220 (2019) 235–252. doi:https://doi.org/10.1016/j.jclepro.2019.02.122.

[6] E.-I.E.-I. Yang, S.-T.S.-T. Yi, Y.-M.Y.-M. Leem, Effect of oyster shell substituted for fine aggregate on concrete characteristics: Part I. Fundamental properties, Cem. Concr. Res. 35 (2005) 2175–2182. doi:10.1016/j.cemconres.2005.03.016.

[7] F. Soltanzadeh, M. Emam-Jomeh, A. Edalat-Behbahani, Z. Soltan-Zadeh, Development and characterization of blended cements containing seashell powder, Constr. Build. Mater. 161 (2018) 292–304. doi:10.1016/J.CONBUILDMAT.2017.11.111.

[8] P. Lertwattanaruk, N. Makul, C. Siripattarapravat, Utilization of ground waste seashells in cement mortars for masonry and plastering, J. Environ. Manage. 111 (2012) 133–141. doi:10.1016/j.jenvman.2012.06.032.

[9] H. Yoon, Oyster Shell as Substitute for Aggregate in Mortar, Waste Manag. Res. 22 (2004) 158–

170. doi:10.1177/0734242X04042456.

[10] H.Y. Wang, W. Ten Kuo, C.C. Lin, C. Po-Yo, Study of the material properties of fly ash added to oyster cement mortar, Constr. Build. Mater. 41 (2013) 532–537. doi:10.1016/j.conbuildmat.2012.11.021.

[11] C. Martínez-García, B. González-Fonteboa, D. Carro- López, F. Martínez-Abella, Recycled mollusc shells., in: J. de Brito, F. Agrela (Eds.), New Trends Eco-Efficient Rcycled Concr., Woodhead Publishing, 2018: pp. 191–204.

[12] C. Martínez-García, B. González-Fonteboa, F. Martínez-Abella, D. Carro- López, Performance of mussel shell as aggregate in plain concrete, Constr. Build. Mater. 139 (2017) 570–583. doi:10.1016/j.conbuildmat.2016.09.091.

[13] C. Martínez-García, B. González-Fonteboa, D. Carro-López, F. Martínez-Abella, Design and properties of cement coating with mussel shell fine aggregate, Constr. Build. Mater. 215 (2019) 494–507. doi:10.1016/j.conbuildmat.2019.04.211.

[14] C. Martínez-García, B. González-Fonteboa, D. Carro-López, F. Martínez-Abella, Impact of mussel shell aggregates on air lime mortars. Pore structure and carbonation, J. Clean. Prod. 215 (2019) 650–668. doi:10.1016/j.jclepro.2019.01.121.

[15] A.O. Pintea, D.L. Manea, New types of mortars obtained by aditiving traditional mortars with natural polymers to increase physico-mechanical performances, Procedia Manuf. 32 (2019) 201–207. doi:https://doi.org/10.1016/j.promfg.2019.02.203.

[16] P. Zhao, M.D. Jackson, Y. Zhang, G. Li, P.J.M. Monteiro, L. Yang, Material characteristics of ancient Chinese lime binder and experimental reproductions with organic admixtures, Constr. Build. Mater. 84 (2015) 477–488. doi:https://doi.org/10.1016/j.conbuildmat.2015.03.065.

[17] S. Fang, H. Zhang, B. Zhang, G. Li, A study of Tung-oil–lime putty—A traditional lime based mortar, Int. J. Adhes. Adhes. 48 (2014) 224–230. doi:10.1016/J.IJADHADH.2013.09.034.

[18] K. Zhang, A. Grimoldi, L. Rampazzi, A. Sansonetti, C. Corti, Contribution of thermal analysis in the characterization of lime-based mortars with oxblood addition, Thermochim. Acta. 678 (2019) 178303. doi:https://doi.org/10.1016/j.tca.2019.178303.

[19] S. Fang, K. Zhang, H. Zhang, B. Zhang, A study of traditional blood lime mortar for restoration of ancient buildings, Cem. Concr. Res. 76 (2015) 232–241. doi:10.1016/j.cemconres.2015.06.006.

[20] G. Wei, H. Zhou, S. Fang, X. Huang, B. Zhang, Effect of lime type on properties of traditional sticky rice-lime mortar, Jianzhu Cailiao Xuebao/Journal Build. Mater. 18 (2015). doi:10.3969/j.issn.1007-9629.2015.05.028.

[21] L. Ventolá, M. Vendrell, P. Giraldez, L. Merino, Traditional organic additives improve lime mortars: New old materials for restoration and building natural stone fabrics, Constr. Build. Mater. 25 (2011) 3313–3318. doi:10.1016/J.CONBUILDMAT.2011.03.020.

[22] R. Alavéz-Ramírez, P. Montes-García, J. Martínez-Reyes, D.C. Altamirano-Juárez, Y. Gochi-Ponce, The use of sugarcane bagasse ash and lime to improve the durability and mechanical properties of compacted soil blocks, Constr. Build. Mater. 34 (2012) 296–305. doi:https://doi.org/10.1016/j.conbuildmat.2012.02.072.

[23] C. Nunes, Z. Slížková, Hydrophobic lime based mortars with linseed oil: Characterization and durability assessment, Cem. Concr. Res. 61–62 (2014) 28–39. doi:10.1016/j.cemconres.2014.03.011.

[24] C. Nunes, Z. Slížková, Freezing and thawing resistance of aerial lime mortar with metakaolin and a traditional water-repellent admixture, Constr. Build. Mater. 114 (2016) 896–905. doi:10.1016/j.conbuildmat.2016.04.029.

[25] C. Nunes, L. Pel, J. Kunecký, Z. Slížková, The influence of the pore structure on the moisture transport in lime plaster-brick systems as studied by NMR, Constr. Build. Mater. 142 (2017) 395–409. doi:10.1016/j.conbuildmat.2017.03.086.

[26] I. Centauro, E. Cantisani, C. Grandin, A. Salvini, S. Vettori, The influence of natural organic

materials on the properties of traditional lime-based mortars, Int. J. Archit. Herit. 11 (2017) 670–684. doi:10.1080/15583058.2017.1287978.

[27] K.A. Gour, R. Ramadoss, T. Selvaraj, Revamping the traditional air lime mortar using the natural polymer – Areca nut for restoration application, Constr. Build. Mater. 164 (2018) 255–264. doi:10.1016/j.conbuildmat.2017.12.056.

[28] P. Pahlavan, S. Manzi, A. Sansonetti, M.C. Bignozzi, Valorization of organic additions in restorative lime mortars: Spent cooking oil and albumen, Constr. Build. Mater. 181 (2018) 650–658. doi:10.1016/j.conbuildmat.2018.06.089.

[29] A. Arizzi, H. Viles, G. Cultrone, Experimental testing of the durability of lime-based mortars used for rendering historic buildings, Constr. Build. Mater. 28 (2012) 807–818. doi:10.1016/j.conbuildmat.2011.10.059.

[30] M. Thomson, J. Lindqvist, J. Elsen, C. Groot, Chapter 2.5 Characterisation: Porosity of mortars, in: 2007: p. 75.

[31] K. Van Balen, B. Bicer-Simsir, L. Binda, C. Bläuer, J. Elsen, C. Groot, E. Hansen, R. Van Hees, F. Henriques, J. Hughes, E.E. Toumbakari, T. Von Konow, J.E. Lindqvist, P. Maurenbrecher, B. Middendorf, I. Papayianni, S. Simon, M. Stefanidou, M. Subercaseaux, C. Tedeschi, M. Thomson, J. Valek, M.R. Valluzi, Y. Vanhellemont, M.R. Veiga, Performance and Repair Requirements for Renders and Plasters, in: 2nd Hist. Mortars Conf. HMC2010 RILEM TC 203-RHM Final Work., Prague, Czech Republic, 2010: pp. 1359–1363.

[32] P. Maravelaki-Kalaitzaki, Hydraulic lime mortars with siloxane for waterproofing historic masonry, Cem. Concr. Res. 37 (2007) 283–290. doi:10.1016/J.CEMCONRES.2006.11.007.

[33] A. Delagrave, J. Marchand, M. Pigeon, Influence of Microstructure on the Tritiated Water Diffusivity of Mortars, Adv. Cem. Based Mater. 7 (1998) 60–65. doi:https://doi.org/10.1016/S1065-7355(97)00029-1.

[34] B.M. Yu, J.H. Li, A geometry model for tortuosity of flow path in porous media, Chinese Phys. Lett.

21 (2004) 1569–1571. doi:10.1088/0256-307X/21/8/044.

[35] M. Matyka, A. Khalili, Z. Koza, Tortuosity-porosity relation in porous media flow, Phys. Rev. E. 78 (2008) 26306. doi:10.1103/PhysRevE.78.026306.

[36] Q. and L.C. Sobieski Wojciechand Zhang, Predicting Tortuosity for Airflow Through Porous Beds Consisting of Randomly Packed Spherical Particles, Transp. Porous Media. 93 (2012) 431–451. doi:10.1007/s11242-012-9961-8.

[37] M. Barrande, R. Bouchet, R. Denoyel, Tortuosity of Porous Particles, Anal. Chem. 79 (2007) 9115–9121. doi:10.1021/ac071377r.

[38] S.A. and H.A.F.A. and T.C. Scholes O. N.and Clayton, Permeability anisotropy due to consolidation of compressible porous media, Transp. Porous Media. 68 (2007) 365–387. doi:10.1007/s11242-006-9048-5.

[39] K. Van Balen, Carbonation reaction of lime, kinetics at ambient temperature, Cem. Concr. Res. 35 (2005) 647–657. doi:10.1016/j.cemconres.2004.06.020.

[40] O. Cazalla, C. Rodriguez-Navarro, E. Sebastian, G. Cultrone, M.J. Torre, Aging of Lime Putty: Effects on Traditional Lime Mortar Carbonation, J. Am. Ceram. Soc. 83 (2004) 1070–1076. doi:10.1111/j.1151-2916.2000.tb01332.x.

[41] C. Nunes, P. Mácová, D. Frankeová, R. Ševčík, A. Viani, Influence of linseed oil on the microstructure and composition of lime and lime-metakaolin pastes after a long curing time, Constr. Build. Mater. 189 (2018) 787–796. doi:10.1016/J.CONBUILDMAT.2018.09.054.

[42] M. Azenha, K. Maekawa, T. Ishida, R. Faria, Drying induced moisture losses from mortar to the environment. Part I: experimental research, Mater. Struct. 40 (2007) 801–811. doi:10.1617/s11527-007-9244-y.

[43] T.D. Gonçalves, V. Brito, L. Pel, Water Vapor Emission From Rigid Mesoporous Materials during the Constant Drying Rate Period, Dry. Technol. 30 (2012) 462–474.

doi:10.1080/07373937.2011.647184.

[44] M.C. de F. Salomão, E. Bauer, C. de S. Kazmierczak, M.C. de F. Salomão, E. Bauer, C. de S. Kazmierczak, Drying parameters of rendering mortars, Ambient. Construído. 18 (2018) 7–19. doi:10.1590/s1678-86212018000200239.

[45] P. Faria, A. Martins, Influence of Air Lime type and Curing Conditions on Lime and Lime-Metakaolin Mortars, in: J. Freitas, V.; Delgado (Ed.), Durab. Build. Mater. Components. Build. Pahology Rehabil., Vol 3, Springer, Berlin, Heidelberg, 2013: pp. 105–126. doi:10.1007/978-3-642-37475-3_5.